

ORIGINAL ARTICLE OPEN ACCESS

The Prostate Microbiome Is Associated With Prostate Size and PSA Level, Independent of Age, in BPH Patients

Alec Sun¹ | Juan Sebastian Rodriguez-Alvarez¹ | Shelby Harper¹  | Prajit Khooblal¹ | Thien Dang¹ | Smita De¹ | Aaron W. Miller^{1,2}

¹Department of Urology, Glickman Urological and Kidney Institute, Cleveland Clinic, Cleveland, Ohio, USA | ²Department of Cardiovascular and Metabolic Sciences, Lerner Research Institute, Cleveland, Ohio, USA

Correspondence: Smita De (des@ccf.org) | Aaron W. Miller (millera25@ccf.org)

Received: 5 November 2024 | **Revised:** 5 March 2025 | **Accepted:** 10 March 2025

Funding: This research was supported by the Endourological Society.

Keywords: computational biology | microbiota | prostatic hyperplasia

ABSTRACT

Background: The etiology of benign prostatic hyperplasia (BPH) is not well understood, though recent literature suggests that the urinary tract microbiome may play a role. We aimed to examine the prostatic microbiome in BPH and its associations with patient characteristics.

Methods: Men undergoing Holmium Laser Enucleation of the Prostate (HoLEP) were recruited if they were over 18 years old and had no history of prostate cancer, prostate surgery, or pelvic radiation. Exclusion criteria included positive preoperative urine culture, bladder stones, or catheter-dependence. Patient characteristics including age, prostate-specific antigen (PSA), American Urological Association symptom score (AUASS), and history of biopsy were recorded. Intraoperatively, prostate tissue was collected from each patient, as well as catheterized urine, urethral swabs, and swabs of the specimen container. Samples underwent DNA extraction, 16S sequencing, and analysis using R statistical software. Associations between bacterial taxonomic diversity and patient characteristics were quantified through Sparcc correlations.

Results: Fifty patients were recruited. Mean age, PSA, prostate size, and AUASS were 67.8 years, 4.0 ng/mL, 108.6 g, and 19.4, respectively. After bioinformatic decontamination of prostate samples, alpha and beta diversity analyses indicated that microbiomes from the prostate, urethra, and urine were all distinct ($p = 0.001$); microbiota from the urine and urethra had higher similarity to each other than that of the prostate. *Campylobacter*, *Caryophanaceae*, *Enterobacter*, and *Senegalimassilia* positively correlated with prostate size or PSA.

Conclusions: The prostatic microbiome is unique and distinct from that of urine and urethra, with several known pathogens positively correlating with prostate size and PSA.

1 | Introduction

Benign prostatic hyperplasia (BPH) is a prevalent condition that, when symptomatic, is marked by bothersome lower urinary tract symptoms (LUTS). More concerning, BPH can result in urinary retention with possible impacts on renal function and infection through bladder outlet obstruction [1, 2]. The

incidence of BPH increases with age, with approximately 70% of men between 60 and 69 years of age being impacted [3]. BPH also has significant direct and indirect socioeconomic impacts. There are currently no updated cost analyses of BPH evaluation and treatment within the United States, however, a 2005 study found that BPH requiring treatment would impact approximately 2.2 million men of working age

Alec Sun and Juan Sebastian Rodriguez-Alvarez contributed equally to this work.

This is an open access article under the terms of the [Creative Commons Attribution-NonCommercial-NoDerivs](https://creativecommons.org/licenses/by-nc-nd/4.0/) License, which permits use and distribution in any medium, provided the original work is properly cited, the use is non-commercial and no modifications or adaptations are made.

© 2025 The Author(s). *The Prostate* published by Wiley Periodicals LLC.

(45–64 years old) with a resulting annual loss of \$3.4 billion in health care expenses and \$500 million in lost workdays [4].

Management of BPH includes both medical and surgical options with current surgical guidelines recommending a size-driven approach. According to the American Urological Association (AUA), Holmium Laser Enucleation of the Prostate (HoLEP) is a size-independent endoscopic surgical treatment option for men with symptomatic BPH who have failed or cannot tolerate medical therapies [5]. The procedure is performed transurethraly by using a holmium laser to enucleate the enlarged prostate adenoma, which is then removed from the bladder using a morcellator. Despite its steep learning curve, HoLEP is rapidly gaining traction as a contender for the gold-standard surgical treatment of BPH [6].

A comprehensive understanding of the etiology and pathophysiology of BPH is currently lacking. Further, the cause of drastic variations in prostate sizes (i.e., 10–500+ grams) remains unclear. A number of factors are thought to contribute to BPH [7], including age, endogenous androgens [7], and inflammation [8]. The Reduction by Dutasteride of Prostate Cancer Events (REDUCE) trial found that a remarkable 77.6% of prostate samples demonstrated evidence of chronic inflammation which clinically correlated to symptomatic LUTS [9]. One promising, though largely unexplored, potential driver of the inflammatory state in BPH involves the prostate microbiome. A few preliminary investigations have suggested that the prostate microbiome may influence pathology such as prostate cancer and BPH [10–12]. In addition, severity of LUTS has been recently shown to be associated with a distinct microbiota of the upper and lower urinary tract within an adult male population [13]. A major limitation with two of these studies [10, 11] is lack of rigorous controls to elucidate specific prostate bacteria, low sample sizes, and a lack of associations between the prostate microbiome and BPH patient characteristics. Thus, in this study we aim to directly define the prostate microbiome in patients with BPH undergoing HoLEP through the paired analysis of multiple sample types for each patient. Further, we quantitatively associate microbiome signatures in the prostate to BPH-specific phenotypes, such as prostate size or prostate-specific antigen (PSA) levels, independent of age.

2 | Materials and Methods

This study was approved by the Cleveland Clinic Institutional Review Board (IRB #22-538). Fifty men undergoing HoLEP for BPH at a single institution were recruited, and written informed consent was obtained. Patients were recruited into three groups based on prostate size according to AUA guidelines [14]: moderate (30–80 g), large (80–150 g), and very large (> 150 g). Inclusion criteria included age of at least 18 years, no evidence of prostate cancer, no prior endoscopic or robotic prostate surgery, no prior pelvic radiation, and ability to provide consent. Patients were excluded if they were catheter-dependent, had bladder calculi, or had preoperative urinary tract infection (UTI) requiring antibiotics. HoLEP was chosen for prostate tissue procurement over other surgical interventions for its minimal cautery effect on prostate tissue, low concern for contamination by skin or rectal flora, and essentially random sampling of prostate tissue via morcellation. Patient

characteristics including age, PSA, history of diabetes, history of prostate biopsy, history of UTI or prostatitis, and estimated prostate size were collected via chart review. Additionally, all patients completed an American Urological Association Symptom Score (AUASS) preoperatively.

2.1 | Sample Collection

All samples for microbiome analyses were collected, processed, and analyzed according to established standards for clinical urobiome studies [15, 16], with a few exceptions, as follows. First, the standards do not include collection of prostate tissue. As such, we followed recommendations to collect tissue as aseptically as possible and swabbed collection cups to assess for potential contamination. Additionally, it is recommended to validate molecular-based results through culture-based approaches; however, multiple studies, including those from our laboratory, have robustly validated that molecular-based results accurately recapitulate the viable microbiome of the urinary tract [17–20]. Following induction of general anesthesia but before initiation of surgery and before administration of peri-operative antibiotics, a distal urethral swab, swab of the sterile specimen container, and catheterized urine sample were obtained to act as contamination controls or for comparative analyses. The HoLEP procedure was then completed using standard technique. All prostate tissue was collected aseptically, and two prostate tissue chips (weighing approximately 10 mg each) were placed into a temperature-controlled container. Samples were transferred, within 4 h, to –80°C for storage before processing for microbiome analyses.

2.2 | DNA Extraction and Sequencing

Samples were prepared for DNA extraction as follows. Prostate samples were combined with a 10% guanidinium chloride buffered solution (Molysis DNA enrichment kit), vortexed, and rested for 5 min at room temperature. This DNA enrichment kit is more effective than other kits in the market to deplete host DNA signatures, acting through chemical lysis of host cells and enzymatic degradation of extracellular DNA [21]. Urine was centrifuged for 5 min at 3000 RPM, and the pellet precipitate was collected for use. Urethral and container swabs were vortexed in sterile water with subsequent centrifuging at 3000 RPM. Subsequently, the pellet was collected for extraction.

All samples, as well as sterile water, were included in each round of DNA extraction (10 samples plus positive and negative). DNA extraction was performed using a semi-automated DNA extraction machine (KingFisher Duo Prime; ThermoFisher Scientific, Waltham, MA, USA), using the standard protocol for urine specimens. Following DNA extraction, samples were then sent to the Microbial Sequencing and Analytics Core at the Cleveland Clinic for high throughput sequencing using 16S rRNA primers targeted to the V4 region of the gene on an Illumina MiSeq machine. Before sequencing, DNA concentrations were quantified before and after PCR amplification for normalization before library prep with the Illumina Nextera XT library kit. Sequence runs were conducted to generate 150 bp, paired-end sequences.

2.3 | Bioinformatic Processing and Data Analysis

The 16S sequencing data, generated from prostate tissue, catheterized urine, urethral swabs, swabs of sterile collection containers, and positive/negative controls were processed in R statistical packages unless otherwise noted. Dada2 [22] was used for quality control of sequences using default parameters, along with bimera removal and amplicon sequence variants (ASV) assignment. A combined database of Silva 138 SSURef [23] and NCBI [24] 16S rRNA was used for ASV assignment. The MSA [25] package was used for ASV alignment, and ASV's were arranged into a maximum likelihood phylogeny in phangorn [26]. The resulting phylogenetic tree was then combined with the ASV table as a Phyloseq [27]. object for further processing. From high quality, annotated ASV's, taxa assigned to chloroplasts, mitochondria, or eukaryotes were removed as dietary or host contaminants. The sequencing depth threshold necessary to adequately capture microbial diversity was calculated in Vegan with a rarefaction analysis, whereby the number of species per sample was calculated at every 100 sequences of depth. The point at which > 90% of samples had a slope of the rarefaction curve < 0.01, was considered the saturation point whereby adding additional sequences would not contribute additional diversity [28]. Samples below this empirically determined depth threshold were removed from further analysis. Contamination removal was performed using Decontam [29] with the negative reagent and swabs of sterile specimen cups controls as the source.

The resulting count table of decontaminated and remaining high-quality reads was normalized using DESeq. 2 [30], which executes a negative binomial Wald test to minimize differences based on sequencing depth, while maintaining rare taxa. From the normalized table, alpha-diversity was next calculated using the phylogenetic diversity metric in Phyloseq. This metric quantifies the number of unique phylogenetic groups in a sample. Beta-diversity was calculated as a weighted UniFrac [31] distance. The weighted UniFrac metric quantifies differences in microbial communities based on presence/absence of phylogenetic groups along with their relative abundance. Beta-diversity statistical analyses were conducted with PERMANOVA, after 999 permutations. Alpha diversity was analyzed using paired *t*-test with Holm's correction, where applicable. The DESeq. 2 algorithm was used to determine which ASV's differentiated samples.

3 | Results

3.1 | Patient Characteristics

Fifty patients underwent HoLEP and were stratified based on prostate size per AUA guidelines [14]—average (30–80 g) ($N=15$), large (80–150 g) ($N=29$), and very large (> 150 g) ($N=6$). Patient characteristics can be seen in Table 1. Mean age was 67.8 years, mean PSA was 4.0 ng/mL, and mean gland size was 108.6 g. LUTS were prevalent, with a mean AUASS of 19.4, which is consistent with moderate-severe symptoms. An average of 64.9 g of prostate tissue was removed during HoLEP, with benign pathology for 49/50 participants; one patient's pathology demonstrated incidental grade group 1 prostatic adenocarcinoma.

TABLE 1 | Baseline characteristics and preoperative BPH symptoms. Demographic information and baseline characteristics were obtained from recruited patients. Patients completed the American Urological Association Symptom Score (AUASS) to grade the severity of their lower urinary tract symptoms. Values expressed as mean (SD) or raw counts (% of cohort).

	Patient cohort ($n = 50$)
Age (years)	67.8 (7.0)
<i>Race</i>	
White	44
Black or African American	4
Other	2
History of prostate biopsy	26
History of diabetes mellitus	8
History of UTI	9
History of prostatitis	3
PSA (ng/mL)	4.0 (2.8)
Prostate size (g)	108.6 (54.6)
AUASS (scored 1–35)	19.4 (5.9)
AUASS—Quality of life (scored 1–6)	4.3 (1.2)
<i>BPH Symptoms</i>	
Frequency (8+ per day)	36 (72%)
Urgency	35 (70%)
Nocturia	30 (60%)
Incontinence	16 (32%)
Slow urinary stream	28 (56%)
Straining to void	18 (36%)
Urinary intermittency	30 (60%)
Dysuria	7 (14%)

3.2 | The Prostate Microbiome Is Unique

A total of 50 samples each of urine, prostate tissue, urethral swabs, and swabs of sterile collection cups were sequenced along with 25 reagent controls and one positive control that contained known proportions of known bacterial species—*Listeria monocytogenes*, *Pseudomonas aeruginosa*, *Bacillus subtilis*, *Escherichia coli*, *Salmonella enterica*, *Saccharomyces cerevisiae*, and *Cryptococcus neoformans* (Zymbiomics). Initially, we generated > 83K sequences per sample to ensure sufficient sequencing depth for all samples. However, after bioinformatic decontamination of all samples using negative controls, patient samples had an average sequencing depth of $18,955 \pm 1400$ sequences. Details on the effect of each quality control step on sequencing depth is provided in Supporting Information S1: Figure S1a, similar to previous reports [32, 33].

Before decontamination, there were significant differences by sample type in alpha diversity (Supporting Information S1: Figure S1b). In posthoc, pairwise comparisons, reagent and sample cup negatives exhibited similar alpha diversity ($p > 0.05$), which were significantly different from each patient sample type. Similar statistical results were obtained in beta diversity analyses, with globally

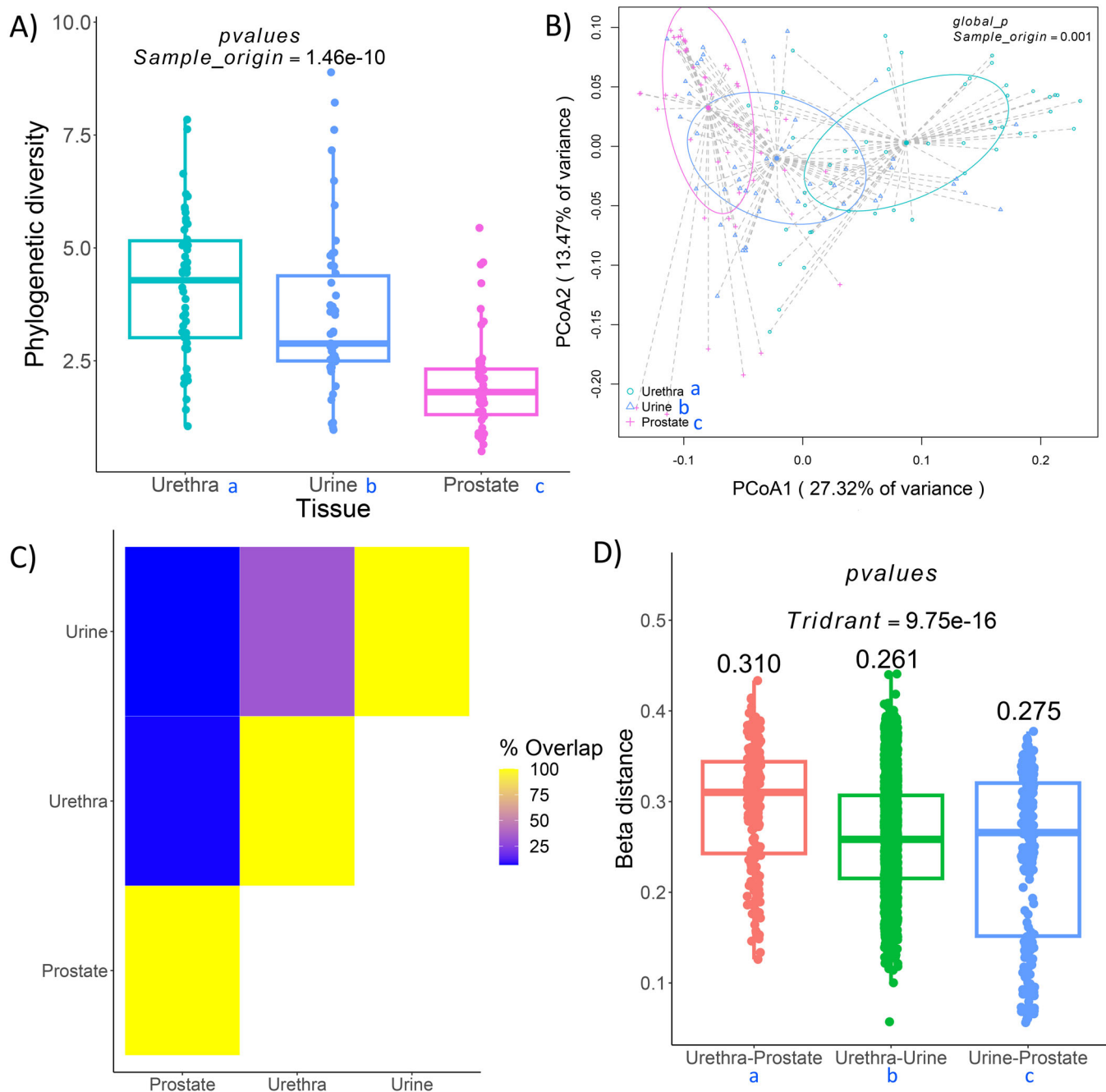


FIGURE 1 | Prostate, urethra, and urinary microbiomes are unique. (A) Phylogenetic diversity of microbiomes by proximity, based on phylogenetic diversity. *p* values reflect one-way ANOVA and blue letters represent statistical groups determined by Holm's-corrected, paired *t*-tests. (B) Weighted UniFrac, dissimilarity analysis of microbiome composition of lower urinary tract samples, by proximity. *p*-Value reflects a one-way PERMANOVA with 999 permutations while blue letters reflect paired PERMANOVA analyses with Holm's corrections. (C) % overlap in ASVs in pairwise comparisons. Data were generated by examining overlap between areas within each patient, which was averaged overall. (D) Between group dissimilarity values. Data are based on all pairwise comparisons. Lower values indicate more similar compositions. *p*-Values reflect one-way ANOVA and blue letters represent statistical groups determined by Holm's-corrected, paired *t*-tests. Blue lettering, where letters are different, represents groups with $p < 0.05$. [Color figure can be viewed at wileyonlinelibrary.com]

significant differences by sample type, driven by significant differences between either the reagent or sample cup negatives and each patient sample type (Supporting Information S1: Figure S1c). On rarefaction analysis, all samples exceeded the saturation point, calculated at < 1000 reads (Supporting Information S1: Figure S1d; blue line). Collectively, data indicate that contamination cannot be an important driver of microbiome results from patient samples.

To further evaluate with environmental contaminants could have contributed to sample data, we quantified the concentration of extracted DNA from all samples and controls, based on QuBit analyses of the DNA. Importantly, the DNA concentration for reagent and swab controls was significantly lower than any tissue samples (Supporting Information S1: Figure S1e), with reagent concentrations ranging from 0.006 to 0.02 ng/ μ L and swab control

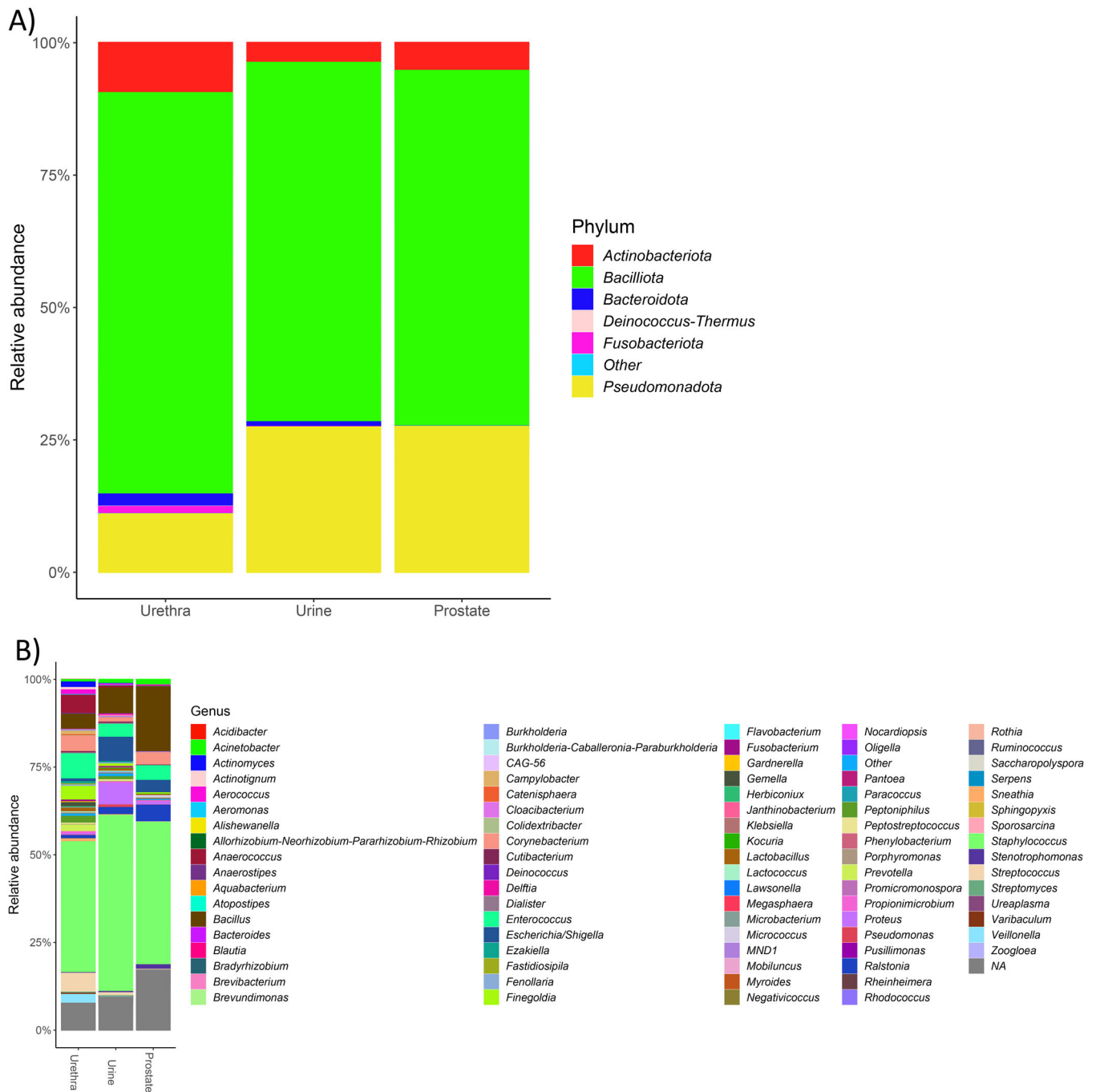


FIGURE 2 | Taxonomic profiles by sample type. (A) Phylum-level profiles. (B) Genus-level profiles. Data reflect the relative abundance of taxa based on the number of sequence counts/sample for each taxon compared to the total number of counts, averaged across all samples. [Color figure can be viewed at wileyonlinelibrary.com]

concentrations ranging from 0.0004 to 0.04 ng/ μ L. The lowest concentration measured in any tissue sample was 0.124 ng/ μ L in urethra, with 90% of samples having concentrations > 2 ng/ μ L. Thus, concentrations for samples in this study were higher than what has been previously reported for the urobiome [34].

Bioinformatic decontamination revealed that 201 of 2485 unique ASV's were identified as contaminants (Supporting Information S2: Table S1). After decontamination, it was revealed that the prostate microbiome exhibited the lowest level of alpha diversity, with significant differences between each sample type (Figure 1A).

Similarly, each sample type exhibited statistically unique microbiome compositions, assessed through beta diversity analysis (Figure 1B). To further validate that the prostate tissue exhibited its own unique microbiome, the overlap in ASV's between urine-urethra, urine-prostate, and prostate-urethra pairs were made for each individual patient and plotted as a heatmap (Figure 1C), which revealed that while the urine and urethra shared > 50% of the same ASV's, the prostate tissue shared < 20% of ASV's with either the urine or urethra. Finally, the beta distance for all sample pairs was calculated, which revealed that the dissimilarity between either the urine or urethra and prostate tissue was significantly higher than

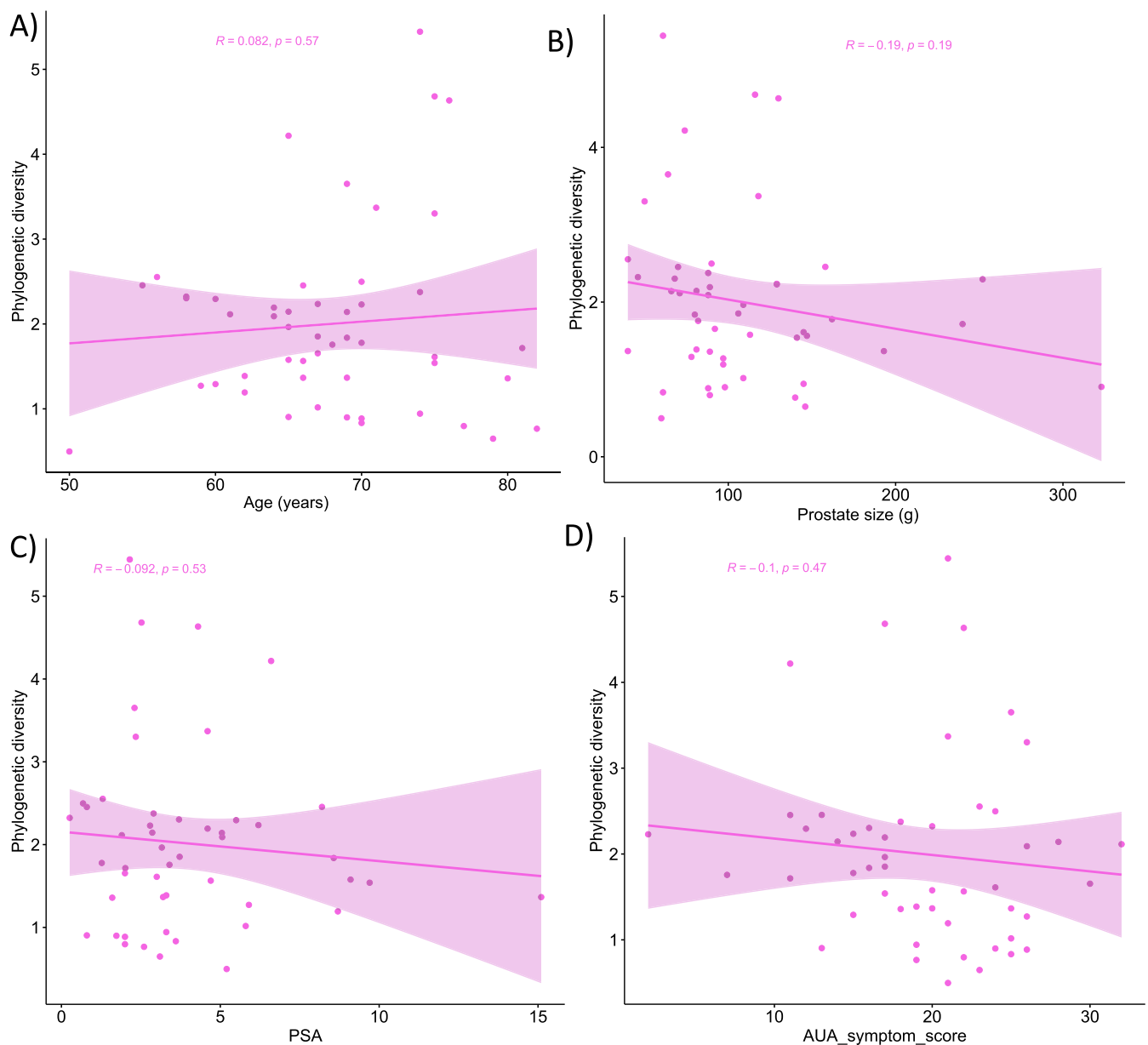


FIGURE 3 | The lower urinary tract does not accumulate diversity over time or with pathology. (A–C) Pearson correlation of phylogenetic diversity in the urine, urethra, and prostate by age (A), prostate size (B), and PSA levels (C). Pearson correlation and p -values are shown for all analyses. [Color figure can be viewed at wileyonlinelibrary.com]

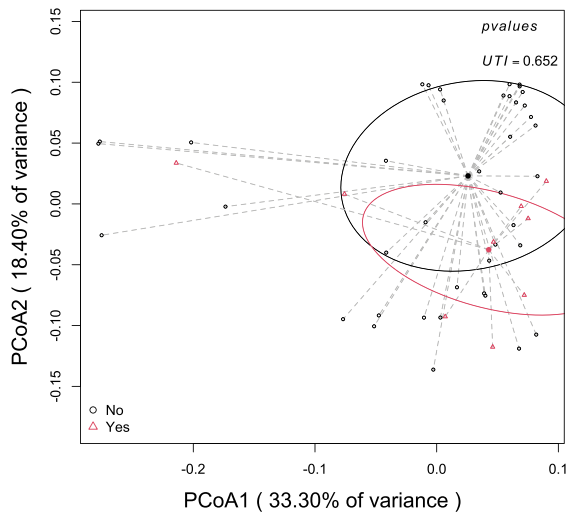
the urine-urethra dissimilarity (Figure 1D). To ensure statistical reliability, the sparseness of the enriched ASV's was evaluated for the 32 ASV's found to correlate to one of the evaluated metrics. The distribution these ASV's among prostate samples ranged from 8% to 100% with 15 ASV's present in > 50% of samples, 8 ASV's present in > 25% of samples, and 9 ASV's present in < 25% of samples (3 of which were present in < 10% of samples). Collectively, these results indicate that the prostate harbors its own unique microbiota different than that found in catheterized urine or urethra.

At the phylum level, Bacillota and Pseudomonadota dominated the microbiomes of urine, urethra, and prostate (Figure 2A), consistent with prior microbiological studies of the lower urinary tract in men [17, 20]. At the genus level, the prostate microbiome again exhibited divergence from the microbiome of the urine or urethra, with a greater abundance of *Bacillus* and not assigned taxa (Figure 2B).

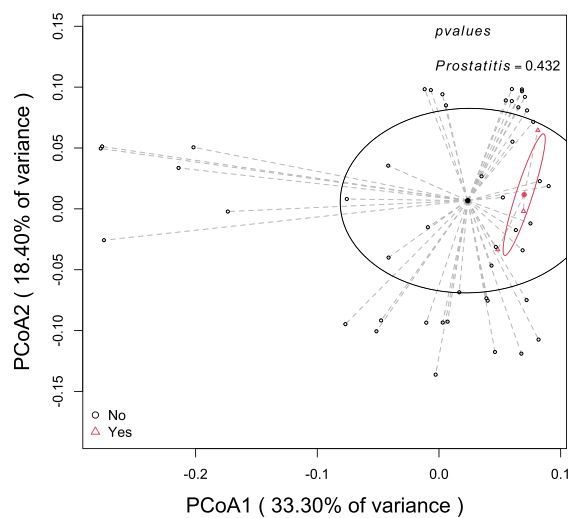
3.3 | Uropathogenic Bacteria Are Associated With Size and PSA

To determine if bacteria accumulated passively in the prostate, we next examined the alpha diversity correlated to age, prostate size, PSA levels, and AUASS, and found no significant correlations (Figure 3A–D). These data indicate that microbiome signatures with BPH are not a result of the passive or stochastic accumulation of bacteria passing through the prostate tissue. Furthermore, beta diversity did not exhibit significant associations with a history of urinary infections, type of perioperative antibiotics used, history of biopsy, or diabetes (Figure 4A–E). However, only three patients exhibited clinical signs of prostatitis, so statistical results for that comparison (Figure 4B) are not reliable. These data indicate that neither infection, type of antibiotics, past surgical interventions (possible source of

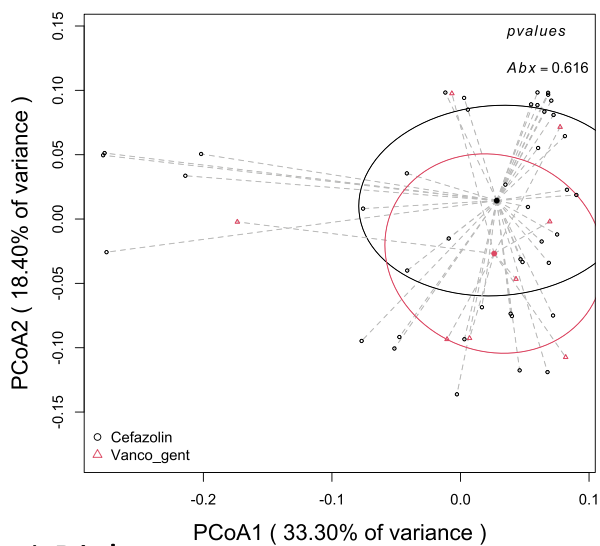
A) UTI



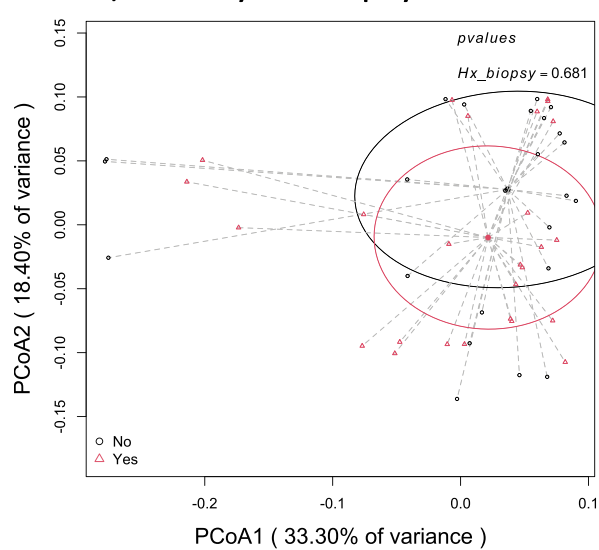
B) Prostatitis



C) Perioperative antibiotics



D) History of biopsy



E) Diabetes

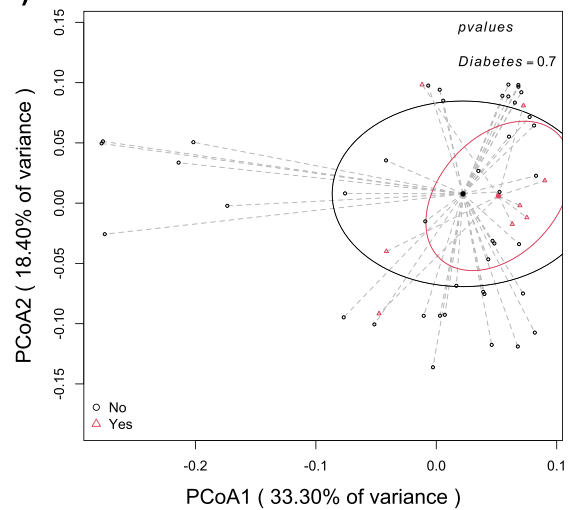


FIGURE 4 | Beta diversity comparisons of clinical metadata. (A) Urinary tract infections, (B) Prostatitis, (C) Perioperative antibiotic choice, (D) History of biopsy, and (E) Diabetes. [Color figure can be viewed at wileyonlinelibrary.com]

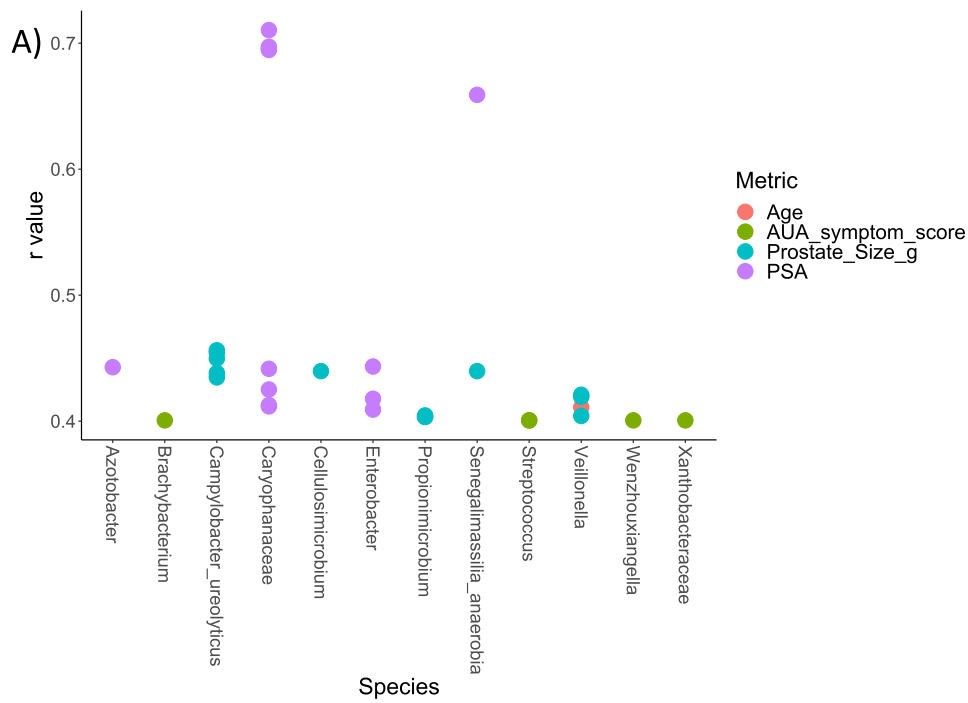


FIGURE 5 | Significant Pearson correlations between normalized sequence counts and age, prostate size, PSA, and AUA symptom score. For all charts, dots represent individuals ASV's, plotted by genus or lowest assigned taxonomy and colored by phylum. [Color figure can be viewed at wileyonlinelibrary.com]

contamination), nor comorbidities are significant drivers of the prostate microbiome signatures.

In contrast to the above results, there were positive correlations between several ASV's and prostate size, PSA, AUASS, and age (Figure 5). Most prominently, *Caryophanaceae* and *Senegalinmassilia* were more strongly positively associated with PSA with *r*-values of 0.7 and 0.65, respectively. Further, several taxa were notably positively associated with prostate size, including *Campylobacter* and *Enterobacter*. Only one ASV exhibited a significant correlation with age, which belonged to the *Veillonella* genus. These data reveal multiple specific taxa, many of which are known uropathogens, are associated with BPH-specific pathologies, independent of age.

4 | Discussion

In the present study, we robustly demonstrated that the BPH prostate harbors a distinct microbiome with several uropathogens noted to be positively correlated with prostate size and PSA. While most prior work has utilized urine for extrapolation of the benign lower urinary tract microbiome, here we directly evaluated prostate tissue while accounting for urethral and urine bacteria to more clearly determine major bacterial players within the prostate microbiome. Additionally, previous studies of the prostate microbiome utilized prostatic fluid or prostate biopsies, collected through the transperineal route [11, 12]. Importantly, the route of prostate biopsies influences the downstream microbiome results, suggesting biopsy induced contaminants [11, 12, 18].

There are few studies assessing the microbiome of prostate tissue directly. Recent work by Chen et al. [12] directly evaluated both

malignant and benign prostate tissue via transperineal biopsy. This is one of the first such studies utilizing appropriate contamination controls. Similarly, we strictly accounted for possible contaminants through urethral and specimen container controls in addition to standard reagent controls (Supporting Information S1: Figure S1). Importantly, our HOLEP surgical approach provided for minimal additional contamination yet allowed for maximal prostatic tissue sampling in comparison to a transurethral biopsy route of sample collection. Furthermore, prostate biopsies necessarily sample the peripheral zone of the prostate whereas we sampled the transitional zone, the overgrowth of which is implicated in bladder outlet obstruction and thus is more relevant when exploring the pathophysiology of BPH. Through the robust negative controls and comparisons with urine and urethral samples on a per patient basis, results collectively indicate the presence of a unique prostate microbiome that cannot be explained by technical contaminants or bacteria passively acquired in the urine or urethra. Our results build on previous research [10] using molecular and fluorescent in situ hybridization approaches to validate the presence of bacteria in human prostate tissue.

As expected, Bacilliota and Pseudomonadota were the dominant phyla found across urine, urethra, and prostate (Figure 2A), with prostate tissue exhibiting an increased abundance of *Bacillus* (Figure 2B) compared to urine and urethral samples. Interestingly, there did not appear to be a strong correlation between overall phylogenetic diversity and prostate size, age, PSA, or AUASS (Figure 3), which suggests that bacteria do not just passively accumulate with age, size, infections, or prior instrumentation. However, several specific bacterial species exhibited significant positive correlations with either prostate size or PSA (Figure 5), including *Campylobacter* or *Enterobacter* which contain species known to be uropathogens or pathobionts. Several identified taxa in this study,

such as *Wenzhouiangella* and *Xanthobacteraceae*, are relatively unknown or with unclear pathogenic potential in humans. Additional work with these taxa may elucidate their importance.

There is limited microbiological evaluation of the diseased prostate, with only one recent study directly exploring microbiome patterns in malignant tissue [12]. In the present study, in addition to evaluating sources of contamination as a driver of prostate microbial signatures, we also sought to evaluate non-BPH influences on the prostate microbiome that included diabetes and UTIs. These diseases, notably, did not appear to influence the overall microbiome within the BPH prostate. Further, while age is known to play a role in the progression of prostate size in BPH, we found only one species that was slightly positively correlated with age (Figure 5). Together, these findings suggest age-independent associations with prostatic hypertrophy, indicative of a potential mechanistic link between these taxa and BPH pathologies.

Our work is limited in that all patient samples were derived from patients undergoing HoLEP. Additionally, we did not validate that microbial signatures were derived from viable bacteria. However, multiple past studies, including those from our laboratory, have consistently found that culture-based analyses of urinary tract sources accurately recapitulate molecular microbiome signatures. Our study is strengthened by several factors. First, we rigorously accounted for possible contamination through use of several contamination controls in addition to standard reagent controls. Additionally, a comparative analysis of urine and urethral microbiomes on a per patient basis revealed a clear prostate microbiome signature and gives credibility that these bacteria may influence prostate physiology. Finally, our strict inclusion criteria may have excluded BPH-pertinent conditions (e.g., urinary retention, prior BPH surgeries) that would provide additional insight into the prostate microbiome seen in BPH.

5 | Conclusion

This study represents the most robust examination of the prostate microbiome in BPH while accounting for multiple sources of contamination. We found a distinct microbiome within the prostate with several uropathogenic bacteria positively associated with prostate size and PSA. This study provides rationale for mechanistic studies to elucidate the role that these identified bacterial species may play in BPH pathogenesis.

Acknowledgments

Alec Sun received the Endourological Society 2022 Summer Scholarship for his work on this project.

Conflicts of Interest

There are no direct conflicts of interest for this study. However, Smita De consults for Boston Scientific and Storz, and is on the advisory board for Andromeda. Aaron Miller has relationships with the National Institutes of Health, Urology Care Foundation, and Coloplast.

Data Availability Statement

The data that support the findings of this study are available from the corresponding author upon reasonable request.

References

1. J. S. Chávez-Iñiguez, G. J. Navarro-Gallardo, R. Medina-González, L. Alcantar-Vallin, and G. García-García, “Acute Kidney Injury Caused by Obstructive Nephropathy,” *International Journal of Nephrology* 2020 (2020): 8846622.
2. J. T. Stoffel, A. C. Peterson, J. S. Sandhu, A. M. Suskind, J. T. Wei, and D. J. Lightner, “AUA White Paper on Nonneurogenic Chronic Urinary Retention: Consensus Definition, Treatment Algorithm, and Outcome End Points,” *Journal of Urology* 198, no. 1 (2017): 153–160.
3. K. B. Egan, “The Epidemiology of Benign Prostatic Hyperplasia Associated With Lower Urinary Tract Symptoms,” *Urologic Clinics of North America* 43, no. 3 (2016): 289–297.
4. C. S. Saigal and G. Joyce, “Economic Costs of Benign Prostatic Hyperplasia in the Private Sector,” *Journal of Urology* 173, no. 4 (2005): 1309–1313.
5. J. S. Sandhu, B. R. Bixler, P. Dahm, et al., “Management of Lower Urinary Tract Symptoms Attributed to Benign Prostatic Hyperplasia (BPH): AUA Guideline Amendment 2023,” *Journal of Urology* 211 (2024): 11–19, <https://doi.org/10.1097/JU.0000000000003698>.
6. A. K. Das, T. M. Han, and T. J. Hardacker, “Holmium Laser Enucleation of the Prostate (HoLEP): Size-Independent Gold Standard for Surgical Management of Benign Prostatic Hyperplasia,” *Canadian Journal of Urology* 27, no. S3 (2020): 44–50.
7. A. Kahokehr and P. J. Gilling, “Landmarks in BPH—From Aetiology to Medical and Surgical Management,” *Nature Reviews Urology* 11, no. 2 (2014): 118–122.
8. G. Theyer, G. Kramer, I. Assmann, et al., “Phenotypic Characterization of Infiltrating Leukocytes in Benign Prostatic Hyperplasia,” *Laboratory Investigation; a Journal of Technical Methods and Pathology* 66, no. 1 (1992): 96–107.
9. J. C. Nickel, C. G. Roehrborn, M. P. O’Leary, D. G. Bostwick, M. C. Somerville, and R. S. Rittmaster, “The Relationship Between Prostate Inflammation and Lower Urinary Tract Symptoms: Examination of Baseline Data From the REDUCE Trial,” *European Urology* 54, no. 6 (December 2008): 1379–1384.
10. K. Okada, K. Takezawa, G. Tsujimura, et al., “Localization and Potential Role of Prostate Microbiota,” *Frontiers in Cellular and Infection Microbiology* 12 (2022): 1048319.
11. H. Yu, H. Meng, F. Zhou, X. Ni, S. Shen, and U. N. Das, “Urinary Microbiota in Patients With Prostate Cancer and Benign Prostatic Hyperplasia,” *Archives of Medical Science* 2, no. 2 (2015): 385–394.
12. V. S. Chen, C. James, M. Khemmani, et al., “A Prospective Evaluation of the Prostate Microbiome in Malignant and Benign Tissue Using Transperineal Biopsy,” *Prostate* 84, no. 13 (2024): 1251–1261.
13. P. Bajic, M. E. Van Kuiken, B. K. Burge, et al., “Male Bladder Microbiome Relates to Lower Urinary Tract Symptoms,” *European Urology Focus* 6, no. 2 (2020): 376–382.
14. L. B. Lerner, K. T. McVary, M. J. Barry, et al., “Management of Lower Urinary Tract Symptoms Attributed to Benign Prostatic Hyperplasia: AUA GUIDELINE PART I—Initial Work-Up and Medical Management,” *Journal of Urology* 206 (2021): 806–817.
15. N. Kachroo, D. Lange, K. L. Penniston, et al., “Standardization of Microbiome Studies for Urolithiasis: An International Consensus Agreement,” *Nature Reviews Urology* 18, no. 5 (2021): 303–311.
16. L. Brubaker, J. P. F. Gourdin, N. Y. Siddiqui, et al., “Forming Consensus to Advance Urobiome Research,” *mSystems* 6, no. 4 (2021): e0137120, <https://doi.org/10.1128/mSystems.01371-20>.
17. G. T. Werneburg, A. Adler, P. Khooblal, et al., “Penile Prostheses Harbor Biofilms Driven by Individual Variability and Manufacturer Even In the Absence of Clinical Infection,” *Journal of Sexual Medicine* 20, no. 12 (2023): 1431–1439.

18. G. T. Werneburg, A. Adler, A. Zhang, et al., “Transperineal Prostate Biopsy is Associated With Lower Tissue Core Pathogen Burden Relative to Transrectal Biopsy: Mechanistic Underpinnings for Lower Infection Risk in the Transperineal Approach,” *Urology* 165 (2022): 1–8.
19. G. T. Werneburg, D. Hettel, S. D. Lundy, et al., “Ureteral Stents Harbor Complex Biofilms With Rich Microbiome-Metabolite Interactions,” *Journal of Urology* 209, no. 5 (2023): 950–962.
20. A. Zampini, A. H. Nguyen, E. Rose, M. Monga, and A. W. Miller, “Defining Dysbiosis in Patients With Urolithiasis,” *Scientific Reports* 9, no. 1 (2019): 5425.
21. P. Rajar, A. Dhariwal, G. Salvadori, et al., “Microbial DNA Extraction of High-Host Content and Low Biomass Samples: Optimized Protocol for Nasopharynx Metagenomic Studies,” *Frontiers in Microbiology* 13 (2022): 1038120.
22. B. J. Callahan, P. J. McMurdie, M. J. Rosen, A. W. Han, A. J. A. Johnson, and S. P. Holmes, “DADA2: High-Resolution Sample Inference From Illumina Amplicon Data,” *Nature Methods* 13, no. 7 (2016): 581–583.
23. C. Quast, E. Pruesse, P. Yilmaz, et al., “The SILVA Ribosomal RNA Gene Database Project: Improved Data Processing and Web-Based Tools,” *Nucleic Acids Research* 41, no. Database issue (2013): 590–596.
24. S. Federhen, “The NCBI Taxonomy Database,” *Nucleic Acids Research* 40, no. Database issue (2012): D136–D143.
25. U. Bodenhofer, E. Bonatesta, C. Horejš-Kainrath, and S. Hochreiter, “msa: An R Package for Multiple Sequence Alignment,” *Bioinformatics* 31, no. 24 (2015): 3997–3999.
26. K. P. Schliep, “Phangorn: Phylogenetic Analysis in R,” *Bioinformatics* 27, no. 4 (2011): 592–593.
27. P. J. McMurdie and S. Holmes, “Phyloseq: A Bioconductor Package for Handling and Analysis of High-Throughput Phylogenetic Sequence Data,” *Pacific Symposium on Biocomputing* (2012): 235–246.
28. M. Witthaus, S. Chawla, D. Puri, et al., “Uropathogenic Dysbiosis Pattern Is Associated With Urethral Fibrosis,” *JU Open Plus* 1, no. 12 (2023): e00080.
29. N. M. Davis, D. M. Proctor, S. P. Holmes, D. A. Relman, and B. J. Callahan, “Simple Statistical Identification and Removal of Contaminant Sequences in Marker-Gene and Metagenomics Data,” *Microbiome* 6, no. 1 (2018): 226.
30. M. I. Love, W. Huber, and S. Anders, “Moderated Estimation of Fold Change and Dispersion for RNA-Seq Data With DESeq. 2,” *Genome Biology* 15, no. 12 (2014): 550.
31. R. G. Wong, J. R. Wu, and G. B. Gloor, “Expanding the UniFrac Toolbox,” *PLoS One* 11, no. 9 (2016): e0161196.
32. N. Kachroo, D. Lange, K. L. Penniston, et al., “Standardization of Microbiome Studies for Urolithiasis: An International Consensus Agreement,” *Nature Reviews Urology* 18, no. 5 (2021): 303–311.
33. L. Brubaker, J. P. F. Gourdine, N. Y. Siddiqui, et al., “Forming Consensus to Advance Urobiome Research,” *mSystems* 6, no. 4 (2021): e0137120.
34. L. Karstens, N. Y. Siddiqui, T. Zaza, A. Barstad, C. L. Amundsen, and T. A. Sysoeva, “Benchmarking DNA Isolation Kits Used in Analyses of the Urinary Microbiome,” *Scientific Reports* 11, no. 1 (2021): 6186.

Supporting Information

Additional supporting information can be found online in the Supporting Information section.